# Heat Capacities at Constant Volume of Pure Water in the Temperature Range 412−693 K at Densities from 250 to 925 kg·m$^{-3}$

**Ilmutdin M. Abdulagatov,* Vasiliy I. Dvoryanchikov, and Abdurakhman N. Kamalov**

Institute for Geothermal Problems of the Dagestan Scientific Center of the Russian Academy of Sciences, 367030 Makhachkala, Kalinina 39 A, Dagestan, Russia

The heat capacity at constant volume $C_V$ of pure water has been measured in the temperature range from 412 K to 693 K at 13 isochores between 250 kg·m$^{-3}$ and 925 kg·m$^{-3}$. Measurements cover the critical region and coexistence curve. Measurements have been made in both the one- and two-phase regions near the phase transition points. The measurements were made in a high-temperature, high-pressure adiabatic nearly constant-volume calorimeter. The uncertainty of the heat capacity measurements is estimated to be within ±2.5%. Liquid and vapor one- ($C'_{V1}$, $C''_{V1}$) and two-phase ($C'_{V2}$, $C''_{V2}$) heat capacities, temperatures ($T_S$), and densities ($\rho_S$) at saturation were obtained by the method of quasi-static thermograms. The parameters ($c$, $T^*$,$V^*$) of the simplified-perturbed-hard-chain-theory (SPHCT) equation of state have been optimized to allow calculations of heat capacities for water in the vapor and liquid phases. The relative average deviations for $H_2O$ were within about ±4.5%, except in the critical region where differences reached 15−20% or more. The two-phase heat capacity data $C_{V2}$ were used to evaluate the second temperature derivatives of the vapor pressure and chemical potential. Values of the vapor pressure of water were calculated from $C_{V2}$ measurements using critical pressure and the temperature derivative of the saturation pressure at the critical point.

## 1. Introduction

Under supercritical conditions, the properties of water are very different from those of ambient water (Franck, 1984). In the supercritical region one obviously has the possibility to vary thermodynamic properties continuously from gaslike to liquidlike values. Water in near-critical and supercritical conditions has special properties, which can make the application interesting beyond the usual use as a solvent. The high compressibility permits substantial and continuous changes of the thermodynamic properties by variation of temperature and pressure only.

Water, the most important solvent in nature, has surprising properties as a reaction medium in its supercritical state. The remarkable anomalous properties of supercritical fluids are widely used in industry. Supercritical fluids are of fundamental importance in geology and mineralogy (for hydrothermal synthesis), in chemistry, in the oil and gas industries (e.g., in tertiary oil recovery), and for some new separation techniques, especially in supercritical fluid extraction (Kiran and Levelt Sengers, 1993; Kiran and Brennecke, 1993; Bright and McNally, 1992; Johnston and Penninger, 1989). Supercritical water is used for destruction of hazardous wastes and has been explored as a solvent medium to carry out chemical reactions or biological degradations without char formation (Modell, 1985; Staszak et al., 1987; Huang et al., 1989; Tester et al., 1991).

Accurate values of the heat capacity are valuable for establishing the behavior of the higher-order temperature derivatives of an equation of state (Amirkhanov et al., 1988; Abdulagatov et al., 1994a,b; Luddecke and Magee, 1996; Weber, 1981). For example, the heat capacity at constant volume $C_V$ is related to the equation of state $P(V, T)$ by

$$\left(\frac{\partial C_V}{\partial V}\right)_T = T\left(\frac{\partial^2 P}{\partial T^2}\right)_V \quad (1)$$

The curvature of $P-T$ isochores are connected with $C_V$ by eq 1.

In addition, the liquid ($C'_{V2}$) and vapor ($C''_{V2}$) saturated heat capacities in the two-phase state are related to the second temperature derivatives ($d^2P_S/dT^2$) and ($d^2\mu/dT^2$) by

$$\frac{d^2P_S}{dT^2} = \frac{C''_{V2} - C'_{V2}}{T(V'' - V')} \quad \text{and} \quad \frac{d^2\mu}{dT^2} = \frac{V''C'_{V2} - V'C''_{V2}}{T(V' - V'')} \quad (2)$$

Therefore, heat capacity measurements are useful contributions to the development of a reliable equation of state. Equations of state whose parameters are determined from $PVT$ measurements in general do not yield a good representation of caloric properties ($C_V$, $C_P$, $H$, $S$) because the calculation depends on the first $(\partial P/\partial T)_V$ and second derivatives $(\partial^2P/\partial T^2)_V$ of the $P-T$ isochores. Values of $(\partial^2P/\partial T^2)_V$ are very small and are often known with low accuracy even when high-quality $P(T, V)$ results are available. If, however, measurements of $C_V$ are available, the use of well-known thermodynamic relations can yield an equation of state that is capable of reproducing caloric ($C_V$, $C_P$, $S$, $H$) and ($P$, $V$, $T$) properties within the experimental accuracy of the measurements. Together with the $PVT$ data, the $C_V$, $V$, $T$ measurements will provide a database for developing improved nonclassical equations of state and testing predictive models for pure water. In this paper the parameters ($c$, $T^*$, $V^*$) of the simplified-perturbed-hard-chain-theory (SPHCT) equation of state have been optimized to calculate the heat capacities for water in the vapor and liquid phases far from the critical point.

In previous papers of Amirkhanov et al. (1974), Kerimov (1964), Baehr et al. (1974), Baehr and Schomacker (1975),

* To whom correspondence should be addressed. E-mail: ilmutdin@boulder.nist.gov or kvadro@sinol.ru.

S0021-9568(98)00046-6 CCC: $15.00 
Published on Web 07/21/1998

**Table 1. Primary Experimental Data for the Specific Heat Capacity at Constant Volume of Pure Water**

| first author | year | density range/kg·m$^{-3}$ | temp range /K |
|---|---|---|---|
| Kerimov | 1964 | 46.210−988.142 | 322.65−773.960 |
| Amirkhanov | 1974 | 45.620−999.001 | 286.69−1021.17 |
| Baehr | 1975 | 212.993−396.04 | 643.15−693.150 |
| Abdulagatov | 1995 | 255.75−426.990 | 643.61−660.870 |
| Abdulagatov | 1998 | 250.00−925.240 | 412.57−693.240 |

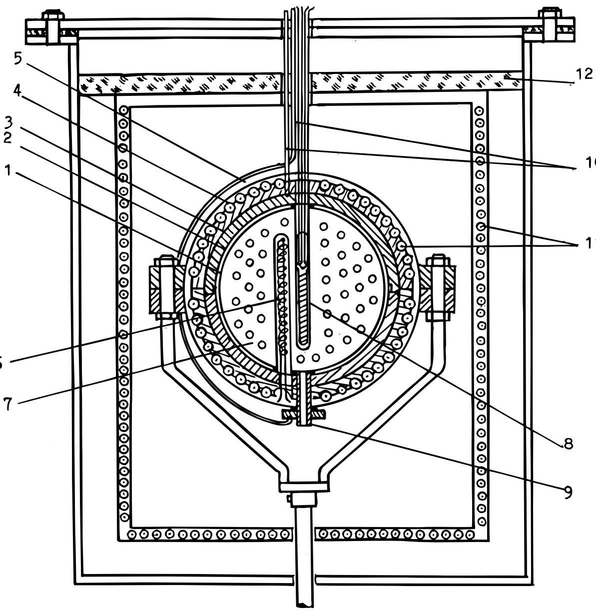


**Figure 1.** Schematic representation of the apparatus for $C_V$ measurements: 1, inner thin-walled spherical bomb; 2, semiconductor layer of $Cu_2O$; 3, 4, 5, outer adiabatic shells; 6, inner heater; 7, perforated stirrer; 8, platinum resistance thermometer; 9, filling pipe; 10, stell tap; 11, outer heaters; 12, asbestos gasket.

and Abdulagatov et al. (1995a), $C_V$ data of pure water at near-critical and supercritical conditions was reported. In Table 1 primary data sets are collected with their individual temperature and density ranges. In Baehr et al. (1974) and Baehr and Schomacker (1975), the $C_V$ data were obtained as the ratio of energy increments $\Delta U$ over temperature increments $\Delta T$, with $\Delta T$ on the order of degrees. In these papers they made measurements of $C_V$ for pure water at nine isochores in the range from (212.993 to 396.040) kg·m$^{-3}$ for temperatures between (643 and 693) K.

In this paper, we report the heat capacity at constant volume of pure water under near-critical and supercritical conditions. The measurements cover the range in temperature from (412 to 693) K at 13 isochores between (250 and 925) kg·m$^{-3}$ which includes the critical region and the coexistence curve.

The apparatus was previously used to measure $C_V$ of pure water, carbon dioxide, ethane, propane, propan-1-ol, propan-2-ol, and binary systems of ethane + propane, $H_2O$ + NaCl, $H_2O$ + KCl, $H_2O$ + NaOH, and $H_2O$ + $KNO_3$ near the critical point of pure water (Abdulagatov et al., 1989, 1993, 1994a,b, 1995a,b, 1996, 1997a,b).

## Experimental Section

The heat capacity at constant volume measurements were performed in the nearly constant-volume adiabatic calorimeter described by Abdulagatov et al. (1997a,b). Briefly, a sample of well-established mass ($m$) is confined to a thin-walled (1.5 mm wall thickness) spherical bomb (diameter 96 mm) of approximately 407.148 cm$^3$ volume.

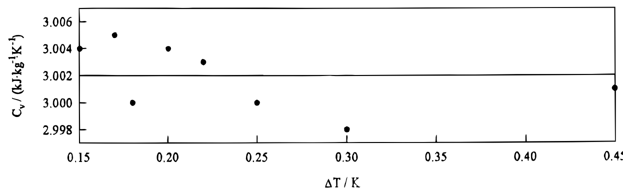


**Figure 2.** Measured heat capacities as a function of the temperature difference $\Delta T$ for isochore $\rho$ = 580.99 kg·m$^{-3}$ at temperature $T$ = 623.8 K.

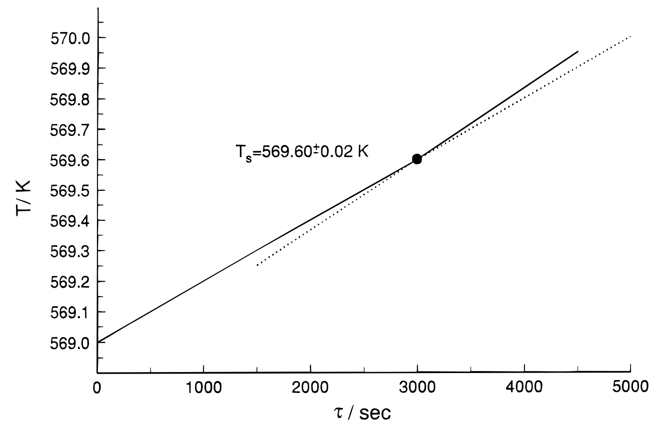


**Figure 3.** Schematic representation of the $T(\tau)$ thermogram for $H_2O$ at isochore 720.046 kg·m$^{-3}$; ●, break point ($T_S$ = 569.60 ± 0.02 K is the coexistence temperature).

The exact volume varies with temperature and pressure. Figure 1 illustrates the scheme of the apparatus. Essentially the calorimetric device consists of the inner bomb, the outer spherical shell (8 mm wall thickness), thermostating screen, high-precision temperature regulator for the thermostat and for the adiabatic layer shell, calorimetric heater, stirring branch, digital measuring units for power measurement of the calorimetric heater, platinum resistance thermometer (PRT), and filling capillary. In the gap between the inner thin-walled sphere and the outer shell the highly sensitive semiconducting material (copper oxide $Cu_2O$) was situated. A layer of $Cu_2O$ ensured adiabatic protection and acted as a thermal screen and performed the role of a layer transmitting pressure to a stronger outer shell. By using a sensitive potentiometer, it was possible to control the temperature differences between the inner sphere and the first thermal screen with an accuracy of $\pm 10^{-5}$ K. This permitted reduction of heat losses through the semiconductor layer to a minimum. The outer heater offered the possibility of regulating the temperature of the outer shell, keeping it constant at the temperature of the inside part of the calorimeter.

When a precisely measured amount of electrical energy ($\Delta Q$) is applied, the resulting temperature rise ($\Delta T$) is measured. When the empty-calorimeter heat capacity $C_0$ is subtracted from the total heat capacity ($\Delta Q/\Delta T$), the heat capacity of the sample is

$$C_V = \frac{1}{m}\left\{\frac{\Delta Q}{\Delta T} - C_0\right\} \qquad (3)$$

The empty-calorimeter heat-capacity $C_0$ was previously determined using different standard liquids with a well-known heat capacity at constant pressure at atmospheric pressure (water, heptane, and hexane) (Vargaftik, 1983) in the temperature range from (293 K to 700 K). The scatter of the experimental results was not larger than ±0.3%. For our calorimeter heat capacity of the empty

**Table 2. Experimental Values of Heat Capacities $C_V$ for Pure Water in the One- and Two-Phase Region at Various Isochories as a Function of Temperature**

| $T$/K | $C_V$/kJ·kg$^{-1}$·K$^{-1}$ |
|---|---|
| $\rho$ = 925.241/kg·m$^{-3}$ | |
| two-phase | |
| 412.536 | 4.274 |
| 412.936 | 4.275 |
| 413.326 | 4.276 |
| 413.726 | 4.275 |
| 414.116 | 4.275 |
| one-phase | |
| 414.509 | 3.606 |
| 414.906 | 3.608 |
| 415.296 | 3.607 |
| 415.696 | 3.606 |
| 416.085 | 3.606 |
| 416.475 | 3.605 |
| $\rho$ = 913.993/kg·m$^{-3}$ | |
| two-phase | |
| 424.764 | 4.307 |
| 425.154 | 4.308 |
| 425.544 | 4.307 |
| 425.924 | 4.307 |
| 426.314 | 4.307 |
| 426.704 | 3.537 |
| one-phase | |
| 427.084 | 3.538 |
| 427.484 | 3.538 |
| 427.864 | 3.537 |
| 428.254 | 3.536 |
| 428.644 | 3.536 |
| 429.023 | 3.537 |
| 429.413 | 3.536 |
| $\rho$ = 874.738/kg·m$^{-3}$ | |
| two-phase | |
| 462.401 | 4.437 |
| 462.771 | 4.437 |
| 463.141 | 4.437 |
| 463.521 | 4.438 |
| 464.261 | 4.439 |
| one-phase | |
| 464.631 | 3.407 |
| 465.001 | 3.403 |
| 465.381 | 3.412 |
| 465.751 | 3.415 |
| 466.121 | 3.403 |
| 466.851 | 3.395 |
| $\rho$ = 807.037/kg·m$^{-3}$ | |
| two-phase | |
| 516.330 | 4.693 |
| 516.690 | 4.693 |
| 517.040 | 4.694 |
| 517.400 | 4.694 |
| 517.750 | 4.694 |
| one-phase | |
| 518.100 | 3.185 |
| 518.450 | 3.181 |
| 518.810 | 3.189 |
| 519.150 | 3.181 |
| 519.510 | 3.177 |
| 519.860 | 3.181 |
| 520.210 | 3.173 |
| $\rho$ = 720.046/kg·m$^{-3}$ | |
| two-phase | |
| 567.701 | 5.161 |
| 568.041 | 5.161 |
| 568.371 | 5.154 |
| 568.711 | 5.155 |
| 569.051 | 5.159 |
| 569.391 | 5.163 |
| one-phase | |
| 569.731 | 3.030 |
| 570.051 | 3.030 |
| 570.391 | 3.028 |
| 570.731 | 3.027 |
| 571.071 | 3.026 |
| 571.411 | 3.028 |

| $T$/K | $C_V$/kJ·kg$^{-1}$·K$^{-1}$ |
|---|---|
| $\rho$ = 580.990 /kg·m$^{-3}$ | |
| two-phase | |
| 619.099 | 6.045 |
| 619.409 | 6.048 |
| 619.739 | 6.061 |
| 620.069 | 6.046 |
| 620.389 | 6.052 |
| 620.719 | 6.061 |
| 621.379 | 6.070 |
| one-phase | |
| 621.709 | 3.018 |
| 622.029 | 3.022 |
| 622.679 | 3.031 |
| 623.009 | 3.031 |
| 623.759 | 3.002 |
| 624.089 | 3.005 |
| 624.409 | 2.998 |
| $\rho$ = 455.560/kg·m$^{-3}$ | |
| two-phase | |
| 640.247 | 8.183 |
| 640.577 | 8.187 |
| 640.897 | 8.180 |
| 641.537 | 8.187 |
| 641.867 | 8.200 |
| 642.187 | 8.229 |
| 642.507 | 8.208 |
| 642.827 | 8.246 |
| 643.147 | 8.313 |
| one-phase | |
| 643.467 | 3.214 |
| 643.787 | 3.198 |
| 644.117 | 3.189 |
| 644.437 | 3.202 |
| 644.757 | 3.198 |
| 645.077 | 3.185 |
| 645.727 | 3.173 |
| $\rho$ = 424.863/kg·m$^{-3}$ | |
| two-phase | |
| 643.207 | 8.207 |
| 643.847 | 8.297 |
| 644.167 | 8.361 |
| 644.487 | 8.503 |
| 644.817 | 8.693 |
| 645.137 | 9.310 |
| one-phase | |
| 645.457 | 3.474 |
| 645.777 | 3.471 |
| 646.106 | 3.469 |
| 646.426 | 3.461 |
| 646.746 | 3.438 |
| 647.066 | 3.421 |
| 647.386 | 3.401 |
| 647.706 | 3.404 |
| 648.036 | 3.394 |
| 648.676 | 3.387 |

| $T$/K | $C_V$/kJ·kg$^{-1}$·K$^{-1}$ |
|---|---|
| $\rho$ = 370.370/kg·m$^{-3}$ | |
| two-phase | |
| 644.247 | 9.331 |
| 644.887 | 9.542 |
| 645.207 | 9.736 |
| 645.537 | 9.875 |
| 645.856 | 10.113 |
| 646.176 | 10.397 |
| 646.496 | 10.632 |
| 646.576 | 10.970 |
| 646.666 | 11.110 |
| 646.746 | 11.595 |
| 646.826 | 12.105 |
| 646.896 | 13.189 |
| one-phase | |
| 647.976 | 6.191 |
| 647.146 | 5.680 |
| 647.306 | 5.341 |
| 647.466 | 5.211 |
| 647.626 | 4.703 |
| 647.786 | 4.902 |
| 647.946 | 4.847 |
| 648.106 | 4.779 |
| 648.426 | 4.605 |
| 648.746 | 4.520 |
| 649.066 | 4.437 |
| 649.386 | 4.356 |
| 649.706 | 4.286 |
| 650.026 | 4.235 |
| 650.346 | 4.190 |
| 650.665 | 4.148 |
| 651.985 | 4.084 |
| 651.305 | 4.068 |
| 651.625 | 3.968 |
| 651.945 | 3.951 |
| 652.265 | 3.867 |
| 652.905 | 3.855 |
| 653.225 | 3.846 |
| 660.884 | 3.680 |
| 661.204 | 3.708 |
| 661.524 | 3.700 |
| 661.834 | 3.691 |
| 662.154 | 3.667 |
| 662.474 | 3.654 |
| 662.794 | 3.654 |
| 663.114 | 3.608 |
| 663.424 | 3.653 |
| 663.744 | 3.657 |
| 664.064 | 3.604 |
| 664.384 | 3.600 |
| 672.602 | 3.546 |
| 672.912 | 3.520 |
| 673.232 | 3.506 |
| 673.542 | 3.507 |
| 673.862 | 3.520 |
| 674.182 | 3.511 |

| $T$/K | $C_V$/kJ·kg$^{-1}$·K$^{-1}$ |
|---|---|
| $\rho$ = 344.828/kg·m$^{-3}$ | |
| two-phase | |
| 644.247 | 10.051 |
| 644.567 | 10.180 |
| 644.887 | 10.448 |
| 645.207 | 10.665 |
| 645.537 | 10.929 |
| 645.857 | 11.218 |
| 646.176 | 11.737 |
| 646.496 | 12.311 |
| 646.816 | 13.499 |
| 646.976 | 14.177 |
| 647.146 | 14.877 |
| one-phase | |
| 647.306 | 9.163 |
| 647.466 | 6.932 |
| 647.626 | 6.722 |
| 647.786 | 6.329 |
| 647.946 | 5.902 |
| 648.106 | 5.601 |
| 648.266 | 5.530 |
| 648.426 | 5.400 |
| 648.586 | 5.199 |
| 648.746 | 5.107 |
| 648.906 | 5.151 |
| 649.066 | 4.994 |
| 649.226 | 4.847 |
| 649.386 | 4.772 |
| 649.706 | 4.696 |
| 650.026 | 4.692 |
| 650.186 | 4.579 |
| 650.346 | 4.546 |
| 650.666 | 4.513 |
| 650.985 | 4.499 |
| 651.305 | 4.387 |
| 651.625 | 4.324 |
| 651.945 | 4.274 |
| 652.265 | 4.236 |
| 652.425 | 4.203 |
| 652.585 | 4.190 |
| 652.905 | 4.157 |
| 653.225 | 4.140 |
| 661.204 | 3.859 |
| 661.524 | 3.847 |
| 661.834 | 3.851 |
| 662.154 | 3.835 |
| 662.474 | 3.818 |
| 662.794 | 3.817 |
| 663.114 | 3.793 |
| 663.424 | 3.805 |
| 663.744 | 3.800 |
| 671.022 | 3.688 |
| 671.332 | 3.675 |
| 671.652 | 3.650 |
| 672.962 | 3.666 |
| 672.282 | 3.650 |
| 672.912 | 3.617 |
| 673.232 | 3.646 |
| 673.542 | 3.633 |
| 673.862 | 3.608 |
| 674.182 | 3.616 |

| $T$/K | $C_V$/kJ·kg$^{-1}$·K$^{-1}$ |
|---|---|
| $\rho$ = 316.840/kg·m$^{-3}$ | |
| two-phase | |
| 643.227 | 10.301 |
| 643.547 | 10.206 |
| 643.707 | 10.531 |
| 644.487 | 11.269 |
| 644.807 | 11.800 |
| 645.127 | 12.018 |
| 645.287 | 11.453 |
| 645.447 | 11.453 |
| 645.767 | 12.700 |
| 646.086 | 12.072 |
| 646.406 | 13.094 |
| 646.566 | 13.642 |
| 646.726 | 13.454 |
| 646.886 | 14.990 |
| 647.046 | 15.914 |
| 647.126 | 21.133 |
| 647.206 | 20.025 |
| one-phase | |
| 647.286 | 10.025 |
| 647.366 | 8.125 |
| 647.446 | 7.233 |
| 647.606 | 6.622 |
| 647.766 | 6.145 |
| 647.926 | 6.216 |
| 648.086 | 6.069 |
| 648.246 | 5.894 |
| 648.406 | 5.596 |
| 649.026 | 5.115 |
| 649.186 | 5.190 |
| 649.346 | 5.190 |
| 649.506 | 5.136 |
| 649.666 | 4.935 |
| 650.206 | 4.776 |
| 650.306 | 4.843 |
| 650.466 | 4.688 |
| 650.626 | 4.667 |
| 650.786 | 4.571 |
| 650.945 | 4.566 |
| 651.105 | 4.512 |
| 651.265 | 4.562 |
| 651.595 | 4.412 |
| 651.915 | 4.479 |
| 652.235 | 4.315 |
| 652.395 | 4.349 |
| 652.555 | 4.353 |
| 652.875 | 4.274 |
| 653.035 | 4.257 |
| 653.195 | 4.273 |
| 660.074 | 3.939 |
| 660.234 | 3.926 |
| 660.394 | 3.918 |
| 660.714 | 3.934 |
| 661.034 | 3.934 |
| 661.674 | 3.906 |
| 661.994 | 3.926 |
| 662.154 | 3.914 |
| 662.474 | 3.906 |
| 668.833 | 3.759 |
| 669.153 | 3.759 |
| 675.161 | 3.638 |
| 675.321 | 3.629 |
| 675.641 | 3.613 |
| 675.961 | 3.608 |
| 676.601 | 3.629 |
| 676.761 | 3.641 |
| 676.921 | 3.598 |
| 677.081 | 3.587 |
| 692.387 | 3.399 |
| 692.707 | 3.407 |
| 693.027 | 3.391 |
| 693.187 | 3.370 |

| $T$/K | $C_V$/kJ·kg$^{-1}$·K$^{-1}$ |
|---|---|
| $\rho$ = 309.598/kg·m$^{-3}$ | |
| two-phase | |
| 643.257 | 10.854 |
| 643.937 | 10.544 |
| 644.287 | 10.708 |
| 644.627 | 11.131 |
| 644.977 | 11.390 |
| 645.317 | 11.574 |
| 645.487 | 11.574 |
| 645.657 | 12.077 |
| 645.827 | 11.985 |
| 645.996 | 12.261 |
| 646.166 | 12.805 |
| 646.336 | 13.625 |
| 646.506 | 13.303 |
| 646.676 | 13.776 |
| 646.846 | 14.794 |
| 647.026 | 19.845 |
| 647.196 | 10.251 |
| one-phase | |
| 647.366 | 6.237 |
| 647.536 | 5.053 |
| 647.706 | 5.061 |
| 647.876 | 5.060 |
| 648.046 | 4.869 |
| 648.386 | 4.869 |
| 648.736 | 4.755 |
| 649.076 | 4.718 |
| 649.416 | 4.621 |
| 649.756 | 4.605 |
| 650.096 | 4.608 |
| 650.446 | 4.582 |
| 650.786 | 4.521 |
| 651.465 | 4.446 |
| $\rho$ = 250.000/kg·m$^{-3}$ | |
| two-phase | |
| 642.527 | 13.194 |
| 642.767 | 12.593 |
| 643.007 | 12.851 |
| 643.247 | 12.990 |
| 643.487 | 13.061 |
| 643.727 | 12.570 |
| 643.967 | 13.173 |
| 644.207 | 14.192 |
| 644.447 | 14.213 |
| 644.687 | 14.292 |
| 644.927 | 14.248 |
| 645.167 | 14.366 |
| 645.407 | 14.318 |
| 645.647 | 14.320 |
| 645.887 | 14.409 |
| 646.126 | 14.518 |
| one-phase | |
| 646.366 | 5.634 |
| 646.606 | 4.751 |
| 646.846 | 4.648 |
| 647.326 | 4.616 |

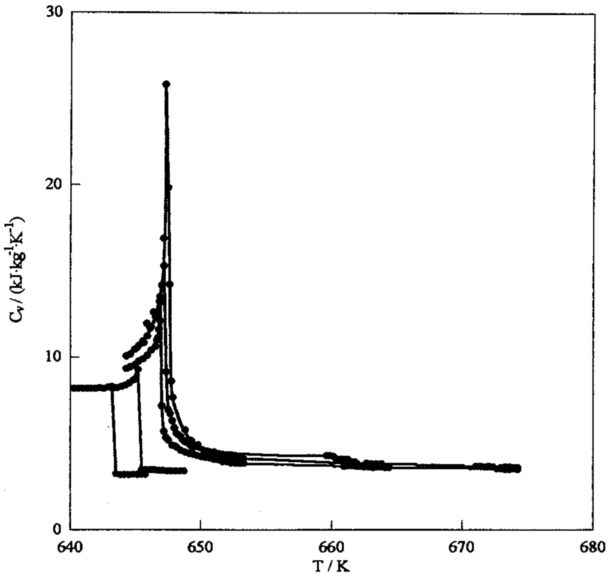


**Figure 4.** Heat capacity at constant volume $C_V$ of the pure water at various liquid isochores as a function of the temperature near the phase transition and critical points. The symbols correspond to the experimental data obtained in this work, and solid curves represent smoothed values of $C_V$.

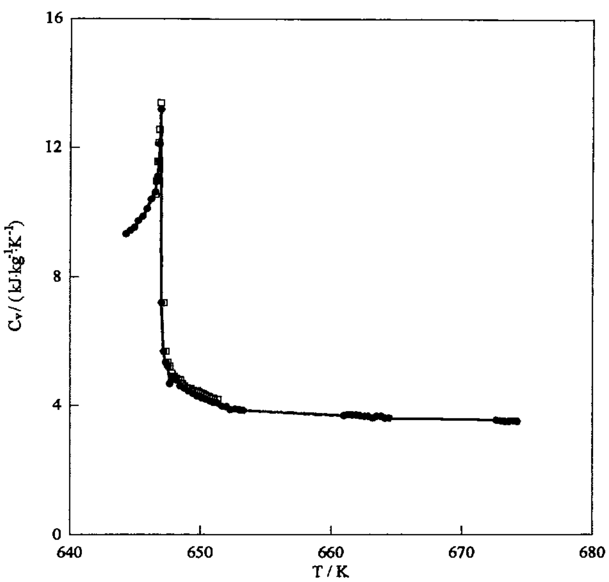


**Figure 5.** Heat capacities at constant volume $C_V$ of $H_2O$ as a function of temperature in the one- and two-phase regions at fixed near-critical isochores $\rho = 370.370$ kg·m$^{-3}$ (□, Kerimov, 1964; ●, this work); the solid line represents smoothed values of $C_V$.

calorimeter could be represented by a linear function of temperature

$$C_0/\text{J·K}^{-1} = 208.724 + 0.127\ T/\text{K} \qquad (4)$$

Uncertainty in $C_V$ measurements arises from several sources. The total uncertainty in reported values for $C_V$ stems from uncertainty in measurement of the quantities $C_0$, $\Delta T$, $m$, and $\Delta Q$ in eq 3.

The relative error in determining the mass of the sample $m$ was ±0.005%. Temperature was measured with a PRT mounted in a tube in the inside of the sphere. The thermometer was calibrated on the IPTS-68. The uncertainty in the temperature measurements was less than ±10 mK.

The density of the sample was determined as the ratio of the mass of the sample $m$ to the working volume $V_{PT}$ of

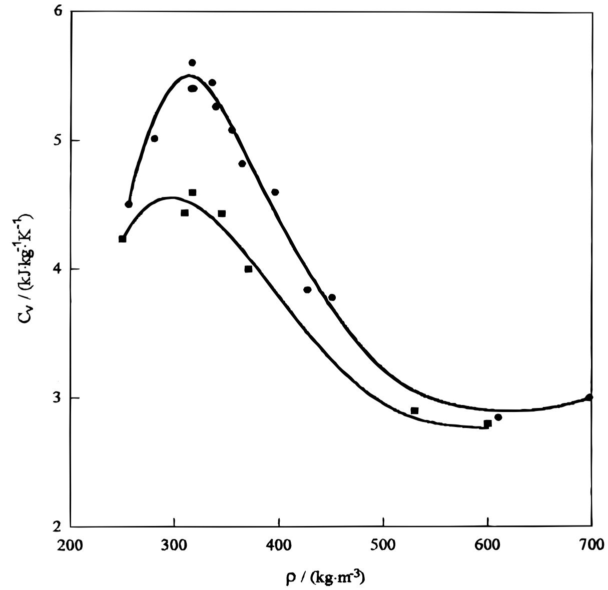


**Figure 6.** The heat capacity at constant volume of pure water at supercritical isotherms as a function of the density. ●, $T = 648.67$ K; ■, $T = 650.73$ K; and the solid line represents smoothed values of $C_V$.

the calorimetric vessel, $\rho = m/V_{PT}$. The volume $V_{PT}$ of the calorimeter was corrected for its variation with temperature $T$ and pressure $P$. Corrections for the volume variations were calculated by an equation discussed previously (Abdulagatov et al., 1997a). The value of this correction to $C_V$ connected with working-volume variation was not larger than ±2% of the total heat capacity.

The average value of the working volume was determined with an uncertainty not exceeding ±0.015%. At selected experimental temperatures $T$ and density $\rho$, the measurements of $C_V$ were performed with different temperature increments $\Delta T$ (from 0.15 to 0.45 K) and energy differences $\Delta Q$ (from 400 to 820 J). Examples of such series of measurements are shown in Figure 2. The measured heat capacities were indeed independent of the applied temperature increment $\Delta T$ and energy differences $\Delta Q$. The uncertainty of the measurements was ±0.3% although applied temperature and energy differences varied by a factor of 3. All measurements in the critical region were made with the samples briefly stirred using a stirrer made of a thin perforated steel foil. This permitted reduction of the errors caused by gravity and achieved homogenization of the investigated sample. The stirring was carried out during 2−3 s by rotating the calorimeter around the vertical axis. The mechanical energy of stirring is negligible.

The greatest uncertainty in the power of the inner heater was estimated to be ±0.1%. Overall accuracy was limited by the fact that $\Delta T$ lay within the bounds ± 2 mK. The heating time was fixed by means of a frequency meter with an accuracy of ±0.001 s.

The heat losses through sections of the calorimetric vessel not controlled by semiconductor ($Cu_2O$) layer were ±0.01%.

For the liquid isochores (large $m$), the uncertainty in $C_V$ is ±1.5%. At vapor isochores (small $m$), the uncertainty in $C_V$ is ±2.5−3%. In the region of the immediate vicinity of the critical point (in the asymptotic region $|\Delta\rho| < 0.25$ and $|\Delta t| < 0.006$) the uncertainty in $C_V$ is ±4.5%.

The measurements were performed in both the forward direction (continuously heating) and in the reverse direction (continuously cooling). The measured isochoric heat

**Table 3. Experimental Values of Temperatures $T_S$, Saturated Densities $\rho_S$, and One-Phase ($C'_{V1}$, $C''_{V1}$)) and Two-Phase ($C'_{V2}$, $C''_{V2}$) Specific Heats for Pure Water**

| $T$/K | $\rho_S$/kg·m$^{-3}$ | $C'_{V2}$/kJ·kg$^{-1}$·K$^{-1}$ | $C'_{V1}$/kJ·kg$^{-1}$·K$^{-1}$ | $C''_{V2}$/kJ·kg$^{-1}$·K$^{-1}$ | $C''_{V1}$/kJ·kg$^{-1}$·K$^{-1}$ |
|---|---|---|---|---|---|
| 414.316 | 925.241 | 4.276 | 3.606 | | |
| 426.504 | 913.993 | 4.308 | 3.538 | | |
| 464.451 | 874.738 | 4.439 | 3.412 | | |
| 517.930 | 807.037 | 4.695 | 3.186 | | |
| 569.561 | 720.046 | 5.164 | 3.031 | | |
| 621.539 | 580.990 | 6.091 | 3.021 | | |
| 642.607 | 455.560 | 8.322 | 3.328 | | |
| 645.297 | 424.860 | 9.341 | 3.579 | | |
| 646.956 | 370.370 | 13.190 | 6.852 | | |
| 647.060 | 344.828 | 17.911 | 9.167 | | |
| 647.095 | 316.850 | | | 34.555 | 21.518 |
| 647.090 | 309.598 | | | 22.140 | 10.300 |
| 646.250 | 250.000 | | | 14.621 | 5.940 |

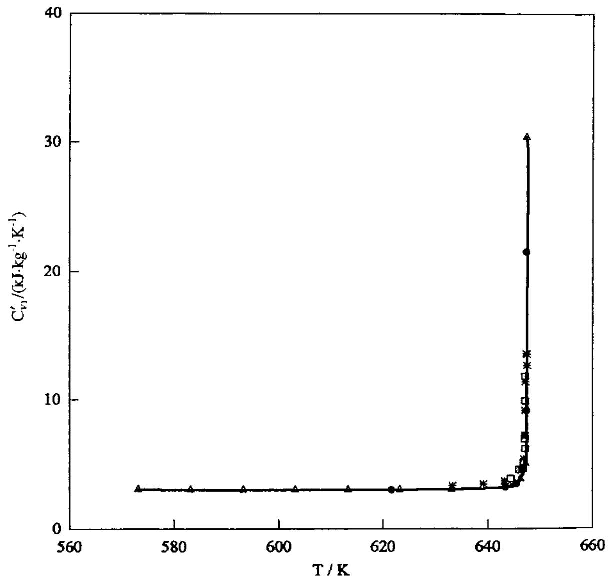


**Figure 7.** One-phase heat capacities at constant volume $C'_{V1}$ of pure water as a function of the temperature on the coexistence curve: ●, this work; *, Abdulagatov et al., 1995; □, Kerimov 1964; △, Amirkhanov et al., 1974; and the solid line represents smoothing values of $C_V$.

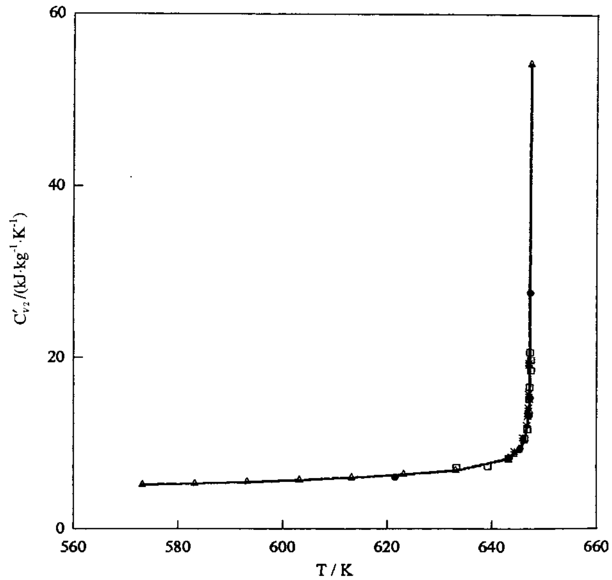


**Figure 8.** Two-phase isochoric heat capacities $C'_{V2}$ of pure water as a function of the temperature on the coexistence curve: ●, this work; *, Abdulagatov et al., 1995; □, Kerimov, 1964; △, Amirkhanov et al., 1974; the solid line represents smoothed values of $C_V$.

capacities $C_V$ are indeed independent of the direction. Differences of the experimental results were not larger than ±0.3%.

The experimental values of saturation temperatures on each isochores was determined by the method of quasi-static thermograms (Voronel, 1974; Abdulagatov et al., 1994b, 1995b, 1997a). After the calorimeter was filled, the temperature was slowly increased with rates $5 \times 10^{-5}$ K/s far from the critical point and $5 \times 10^{-6}$ K/s near the critical point and recorded simultaneously with time ($\tau$) using a graphic recording voltmeter. These $T(\tau)$ thermograms for each isochore showed (Figure 3) a break point at the transition from a two-phase to a homogeneous one-phase region. Each break point was one point on the two-dimensional ($T_S - \rho_S$) phase boundary plane and supplied also a value for the $C'_{V1}$ (one-phase saturated liquid isochoric heat capacity) or $C''_{V1}$ (one-phase saturated vapor isochoric heat capacity) and $C''_{V2}$ (two-phase saturated liquid isochoric heat capacity), or $C''_{V2}$ (two-phase saturated vapor isochoric heat capacity) at this condition. The uncertainty in saturation temperature measured was no worse than ±(0.03 to 0.05) K.

## Results

Thirteen isochores were studied at densities from (250 to 925) kg·m$^{-3}$. Each isochore consists of 11 to 70 points. The temperature range of the results was 412 K to 693 K. In total, 350 $C_V$ measurements were made on 13 isochores, 127 in the two-phase region; and 223 in the one-phase region; 26 values of $C_V$ have been measured on the coexistence curve. The experimental values are given in Table 2. All experimental temperatures were converted to the ITS-90 temperature scale (Preston-Thomas, 1990). Figure 4 presents all our experimental $C_V$ results for isochores as a function of temperature near the phase transition and critical temperatures. Figure 5 shows the experimental behavior of $C_V$ as a function of temperature for $H_2O$ at near-critical isochore. The density dependence of the $C_V$ for pure water at supercritical isotherms $T$ = 648.67 K and $T$ = 650.73 K are given in Figure 6. Values of the one-phase and two-phase heat capacities on the coexistence curve are shown in Figures 7 and 8 together with earlier results. The experimental results of $C_V$ and $T_S - \rho_S$ data on the coexistence curve that were determined by the method of quasi-static thermograms for pure water are presented in Table 3 and Figures 7, 8, and 9. The experimental values of $C_{V2}$ in the two-phase region as a function of volume along the near-critical isotherms presented in Figure 10. As Figure 10 shows, the slope of the two-phase isotherms increases when the critical isotherm is approached. The increasing slope of the isotherms reflects the increase of second temperature derivatives

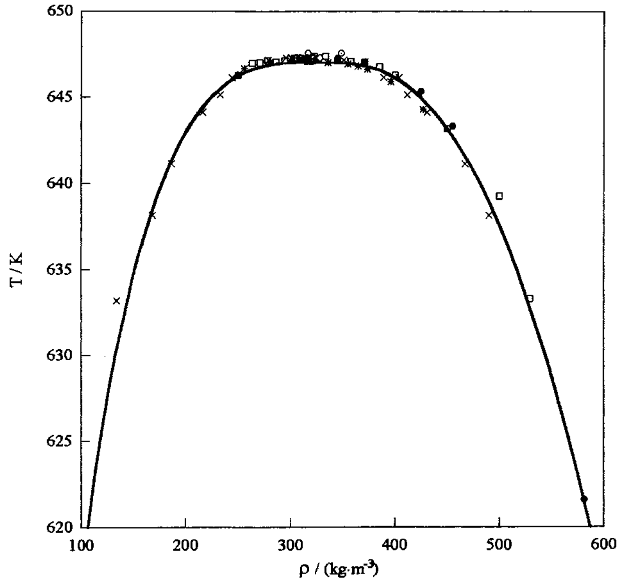


**Figure 9.** Curve of coexisting liquid and vapor densities for pure water: ●, this work; *, Abdulagatov et al., 1995; □, Kerimov, 1964; △, Amirkhanov et al., 1974; solid curve, calculated values from the correlated equation Levelt Sengers 1995.

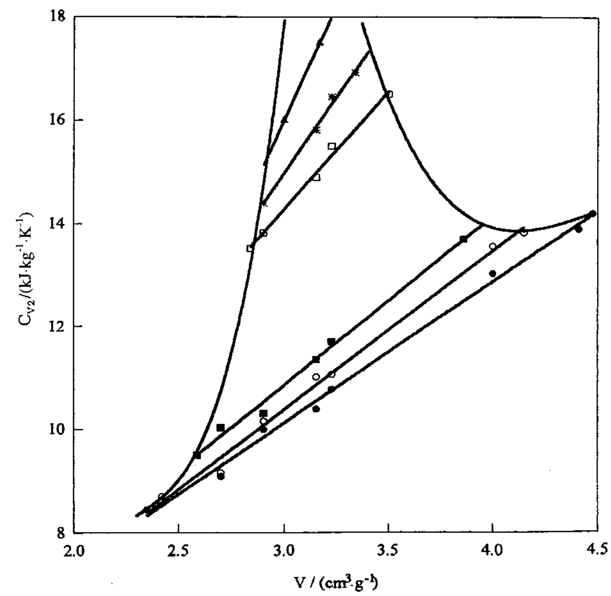


**Figure 10.** Experimental values of $C_{V2}$ in the two-phase region as a function of volume for near-critical isotherms: ●, $T = 644.93$ K; ○, $T = 645.18$ K; ■, $T = 646.54$ K; □, $T = 646.94$ K; *, $T = 647.07$ K; △, $T = 647.09$ K; the solid line represents smoothed values of $C_V$.

$T(d^2P_S/dT^2)$ while the intercept for $V = 0$ is related to $-T(d^2\mu/dT^2)$ (see next section).

## Discussion

In this work the SPHCT model of the equation of state has been used for our $C_V$ experimental results for water. The SPHCT equation of state

$$P = \frac{RT}{V} + \frac{cRT}{V}\cdot\frac{4\eta - 2\eta^2}{(1-\eta)^3} - \frac{RT}{V}\cdot\frac{Z_m cV^*Y}{V + V^*Y}$$

has been applied successfully to the prediction of thermodynamic properties (van Pelt et al., 1992, 1993; Kim et al., 1986). From this equation of state the isochoric heat capacities may be calculated via the relation

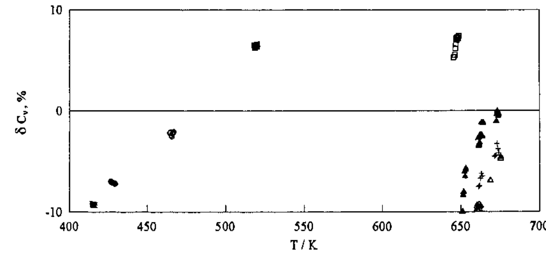


**Figure 11.** Percentage deviations, $\delta C_V = 100(C_V^{exp} - C_V^{cal})/C_V^{exp}$, of the experimental isochoric heat capacity data obtained in this work from the values calculated with the SPHCT model equation of state (eq 5): +, $\rho = 925.241$; ●, $\rho = 913.993$; ○, $\rho = 874.738$; ■, $\rho = 807.037$; □, $\rho = 424.863$; ▲, $\rho = 370.370$; △, $\rho = 344.828$; *, $\rho = 316.840$ kg·m$^{-3}$.

$$C_V = C_{VO}(T) + RZ_m\frac{c(V_r - 1)(Y + 1)}{(V_r + Y)^2}\cdot\left(\frac{1}{2T_r}\right)^2 \qquad (5)$$

where $C_{VO}(T)$ is the ideal-gas heat capacity for water (Vargaftik, 1983)

$$C_{VO}/(\text{J·mol}^{-1}\text{·K}^{-1}) = 25.852\,444\,5 - 0.332\,486 \times 10^{-2}\,(T/\text{K}) + 0.690\,608\,5 \times 10^{-5}(T/\text{K})^2$$

where $V_r = V/V^*$, $T_r = T/T^*$, $Y = \exp(T^*/2T) - 1$, $T^* = \epsilon q/ck$ is the characteristic temperature, $k$ is the Boltzman constant; $Z_m = 18$ is the maximum coordination number, $\epsilon$ is the square-well depth of a surface segment, $V^* = N_A S\sigma^3/\sqrt{2}$ is the molar closet-packed volume, $q$ is the external surface of a molecule, $s$ is the segmental diameter, $S$ is the number of segments per molecule, and $c$ is the Prigogine flexibility parameter. The SPHCT model equation of state contains three molecular parameters $c$, $V^*$, $T^*$. The eq 5 was fitted to the one-phase experimental results in Table 2 in the range far from the critical point. Optimum values of $c$, $V^*$, $T^*$ for water are $c = 1.021 \pm 0.01$; $V^* = 12.825 \pm 0.323$ cm$^3$·mol$^{-1}$; $T^* = 1314.733 \pm 8.946$ K. The deviations between the calculated, eq 5, and experimental data are 4.5−5%. Figure 11 show the relative percentage deviations of the present experimental $C_V$ data for $H_2O$. The maximum of the relative deviations is 10%. In the immediate vicinity of the critical point and the phase transition temperatures, differences increase to about 15−20% or more. For a correct description of the behavior of $C_V$ for water near the critical point, the nonclassical (scaling) equation of state (Levelt Sengers et al., 1983) or the crossover theory (Kiselev et al., 1991; Anisimov and Kiselev, 1992; Kiselev and Sengers, 1993) one must use instead the classical expression (eq 5), which was avoided in these treatments.

Using two-phase heat capacity data $C_{V2}$ the temperature derivatives of vapor pressures and saturated-phase chemical potentials have been extracted on the basis of the Yang−Yang relation

$$\frac{C_{V2}}{T} = -\frac{d^2\mu}{dT^2} + V\frac{d^2P_S}{dT^2} \qquad (6)$$

This relation implies that $C_{V2}$ should be linear versus the volume along each isotherm. For six near-critical isotherms of (644.93, 645.18, 646.54, 646.94, 647.07, 647.09) K, the volume dependence of two-phase heat capacity $C_{V2}$ is shown in Figure 10. This Figure 10 exhibits the linear relationship between the two-phase heat capacity $C_{V2}$ and the volume, the slopes of which equal $T(d^2P_S/dT^2)$ while the intercept for $V = 0$, related to $-T(d^2\mu/dT^2)$. Values of

**Table 4. Comparison of the Vapor Pressure Second Derivatives $d^2P_S/dT^2$ for Pure Water from Heat Capacity Measurements with Values from Published Vapor Pressure Equations**

| $T$/K | $d^2P_S/dT^2$/kPa/K$^2$ [a] | $d^2P_S/dT^2$/kPa/K$^2$ [b] | $d^2P_S/dT^2$/kPa/K$^2$ [c] | $d^2P_S/dT^2$/kPa/K$^2$ [d] | $d^2P_S/dT^2$/kPa/K$^2$ [e] | $d^2\mu/dT^2$/kJ/kg K$^2$ [f] |
|---|---|---|---|---|---|---|
| 644.887 | 4.20 | 3.507 | 3.484 | 3.833 | 3.687 | −0.0032 |
| 645.137 | 4.30 | 3.599 | 3.572 | 3.878 | 3.792 | −0.0034 |
| 646.496 | 5.00 | 4.830 | 4.727 | 4.408 | 4.777 | −0.0018 |
| 646.896 | 6.53 | 7.079 | 6.496 | 5.122 | 5.825 | −0.0026 |
| 647.026 | 12.14 | 13.907 | 9.359 | | | −0.0001 |

[a] This work from $C_V$ measurements. [b] From vapor-pressure equation (Levelt Sengers, 1995). [c] From vapor-pressure equation (Sato et al., 1986). [d] From vapor-pressure equation (Levelt Sengers et al., 1983). [e] From vapor-pressure equation (Levelt Sengers et al., 1972). [f] Values of $d^2\mu/dT^2$ derived in this work from $C_V$ measurements.

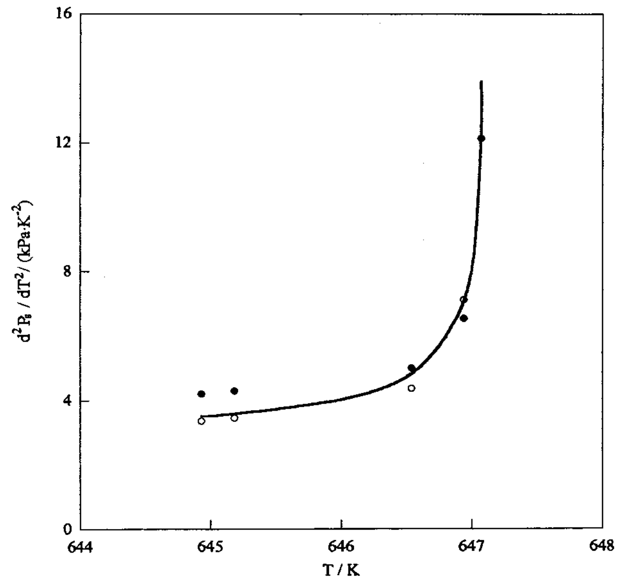


**Figure 12.** Comparison of the vapor-pressure second temperature derivatives ($d^2P_S/dT^2$) from $C_{V2}$ measurements with values from vapor-pressure curve: ●, this work from $C_V$ measurements; ○, Amirkhanov et al., 1974 from $C_V$ measurements; solid line, values calculated from vapor-pressure curve (Levelt Sengers et al., 1983).

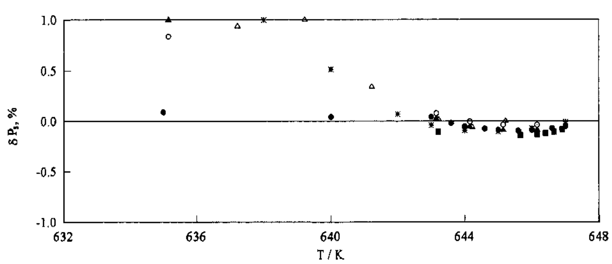


**Figure 13.** Percentage deviations, $\delta P_S = 100(P_S^{(8)} - P_S^{cal})/P_S^{(8)}$, of the vapor-pressure extracted from $C_V$ measurements from the experimental vapor-pressure values and values calculated with vapor-pressure correlating equations: ●, Levelt Sengers et al. (1983); ○, Sato et al. (1986); △, Osborn et al. (1933) (experimental values); ▲, Cooper (1995); *, Wagner et al. (1986); ■, Hanafusa et al. (1986) (experimental values).

$-(d^2\mu/dT^2)$ vary slowly (see Table 4). The results of the calculated values of ($d^2P_S/dT^2$) and ($d^2\mu/dT^2$) from eq 6 for water at each isotherm are given in Table 4 and Figure 12 together with values calculated from various vapor-pressure correlation equations. Values for ($d^2P_S/dT^2$) derived from the $C_{V2}$ data are in reasonable agreement with those derived from the vapor pressure, the differences being within 10−15%. The values of the second temperature derivative ($d^2P_S/dT^2$), determined from our $C_{V2}$ results (Figure 12), increase rapidly as the critical temperature is approached. Methods of extraction of vapor pressures from $C_{V2}$ values are discussed by Abdulagatov et al. (1994a, 1995b, 1997a). The values of adjusting parameters ($P_0$ =

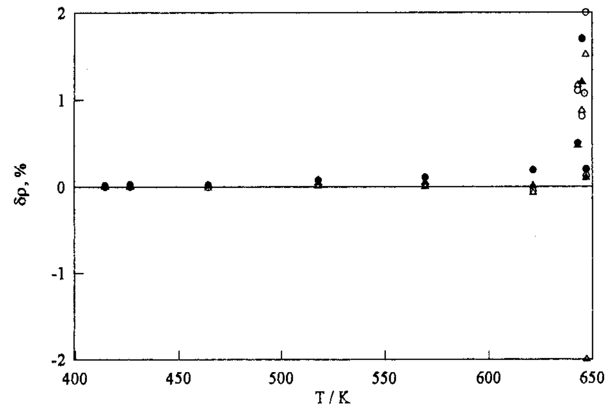


**Figure 14.** Percentage deviations, $\delta\rho_S = 100(\rho_S^{exp} - \rho_S^{cal})/\rho_S^{exp}$, of the saturated vapor−liquid densities derived from $C_V$ measurements from the values calculated with correlation equations: △, Levelt Sengers (1995); ○, Sato et al. (1986); ●, Wagner et al. (1986).

51.2282; $P_1$ = −694.7; $P_2$ = 8655.3817) in the scaling expression

$$\frac{d^2P_S}{dT^2} = \frac{P_C}{T_C^2}\{(1-\alpha)(2-\alpha)P_0t^{-\alpha} + (1-\alpha+\Delta)(2-\alpha+\Delta)P_1t^{\Delta-\alpha} + 6P_2t\} \quad (7)$$

where the critical exponents $\alpha = 0.112$ and $\Delta = 0.5$ and parameters $t = 1 - T/T_C$, $T_C = 647.096$ and $P_C = 22.064$ MPa (Levelt Sengers et al., 1983) have been found from a fit of the eq 7 to the our vapor-pressure second temperature derivatives ($d^2P_S/dT^2$) derived from $C_{V2}$. Integrating eq 7 we obtain the vapor-pressure equation in following form

$$P_S(T) = P_C\left\{1 + \left(\frac{dP_S}{dT}\right)_{cr}t + P_2t^3 + P_0t^{2-\alpha} + P_1t^{2+\Delta-\alpha}\right\} \quad (8)$$

where $(dP_S/dT)_{cr}$ = 7.412 MPa/K. The values of vapor pressures calculated from $C_{V2}$ data (eq 8) using the values of pressure and temperature derivative at critical point show satisfactorily agreement with experimental vapor pressure data in the critical region ($T_C - 10 < T < T_C$. The average relative deviation of $P_S$ is about 0.2−0.3%. A more detailed comparison of vapor-pressure data derived from $C_V$ measurements and the experimental and correlated vapor-pressure values are given in Figure 13. In the temperature range between 642 K and $T_C$ the deviations are within about ±0.1%. The extrapolation to lower temperatures (down to 635 K) results show deviations that reached up to +1.0%. In Figure 14 we also give the results of the comparison of our experimental coexistence vapor−liquid densities data ($\rho'_S$, $\rho''_S$) derived from $C_V$ measurements with values calculated from correlating equations (Levelt Sengers, 1995; Sato et al., 1986; Wagner et al., 1986). The average and maximum of the relative deviations are ±0.2% and +2%.

## Conclusions

New measurements of the isochoric heat capacities of pure water are reported. The measurements were performed in a high-temperature and high-pressure adiabatic nearly constant-volume calorimeter in the temperature range of 412 K to 693 K at densities from (250 to 925) $kg \cdot m^{-3}$ with an uncertainty of ±2%. In this paper we present also the new $C_V$ and $T_S - \rho_S$ measurements of pure water along the coexistence curves in the temperature range from 412 K to 647 K. These measurements include the critical region. The results for the measurements on water are correlated by the classical SPHCT model of the equation of state. The parameters ($c$, $T^*$, $V^*$) of the SPHCT equation of state have been calculated using the new heat capacity measurements for water in the vapor and liquid phases. The relative average deviations for $H_2O$ are within about ±4.5%, except for the critical region where differences reached 15−20% and more. The two-phase heat capacities data $C_{V2}$ were used to evaluate the second temperature derivatives of the vapor pressure and chemical potential. The values of vapor pressure was extracted from $C_{V2}$ measurements using only the pressure and temperature derivative at the critical point.

## Acknowledgment

The authors are very grateful to the Dr. J. W. Magee for his helpful comments, discussion and providing the program for temperature scale conversion from IPTS-68 to ITS-90.

## Literature Cited

Abdulagatov, I. M.; Dvoryanchikov, V. I. Isochoric heat capacity of {$x$H$_2$O + (1 − x)KOH} near the critical point of pure water. *J. Chem. Thermodyn.* **1993**, *25*, 823−830.

Abdulagatov, I. M.; Dvoryanchikov, V. I.; Abdurakhmanov, I. M. Thermodynamic properties of aqueous sodium hydroxide solutions near the liquid−gas critical point. Properties of water and steam. *Proceedings of the 11th International Conference*; Pichal, M., Sifner, O., Eds.; Hemisphere Publishing Corporation: New York, 1989; pp 203−209.

Abdulagatov, I. M.; Polikhronidi, N. G.; Batyrova, R. G. Measurements of the heat capacities $C_v$ of carbon dioxide in the critical region. *J. Chem. Thermodyn.* **1994a**, *26*, 1031−1045.

Abdulagatov, I. M.; Polikhronidi, N. G.; Batyrova, R. G. Isochoric heat capacity and liquid−gas coexistence curve of carbon dioxide in the region of the immediate vicinity of the critical point. *Ber. Bunsen-Ges. Phys. Chem.* **1994b**, *98*, 1068−1072.

Abdulagatov, I. M.; Mursalov, B. A.; Gamzatov, N. M. Pseudospinodal phenomena and scaling of the isochoric heat capacity of the water in the vicinity of the critical point including the metastable region. Physical chemistry of aqueous systems. Proceedings of the 12th International Conference on the Properties of Water and Steam. White, H., Sengers, J. V., Neumann, D. B., Bellows, J. C., Eds.; Begell House: New York, 1995a; pp 94−102.

Abdulagatov, I. M.; Levina. L. N.; Zakaryaev, Z. R.; Mamchenkova, O. N. Thermodynamic properties of propane in the critical region. *J. Chem. Thermodyn.* **1995b**, *27*, 1385−1406.

Abdulagatov, I. M.; Kiselev, S.B.; Levina, L. N.; Zakaryaev, Z. R.; Mamchenkova, O. N. Experimental and theoretical studies of the crossover of the specific heat $C_{v,x}$ of ethane, propane, and their mixture at critical isochores. *Int. J. Thermophys.* **1996**, *17*, 423−440.

Abdulagatov, I. M.; Levina, L. N.; Zakaryaev, Z. R.; Mamchenkova, O. N. The two-phase specific heat at constant volume of propane in the critical region. *Fluid Phase Equilibr.* **1997a**, *127*, 205−236.

Abdulagatov, I. M.; Dvoryanchikov, V. I.; Kamalov, A. N. Measurements of the heat capacities at constant volume of $H_2O$ and $H_2O$ + $KNO_3$. *J. Chem. Thermodyn.* **1997b**, *29*, 1387−1407.

Amirkhanov, Kh. I.; Stepanov, G. V.; Alibekov, B. G. *Isochoric Heat Capacity of Water and Steam*; Amerind Publishing Co.: New Delhi. 1974.

Amirkhanov, Kh. I.; Abdulagatov, I. M.; Alibekov, B. G.; Stepanov, G. V.; Boy, O. A. Equation of state and thermodynamic properties of propan-2-ol. *J. Chem. Thermodyn.* **1988**, *20*, 1385−1406.

Anisimov, M. A.; Kiselev, S. B. *Soviet Technical Review B. Thermal Physics.* Sheidlin, A. E., Fortov, V. E., Eds.; Hardwood Academic: London, 1992; Vol. 3., Part. 2.

Baehr, H. D.; Schomacker, H.; Schulz, S. Experimental determination of the internal energy of water in the vicinity of the critical point. *Forsch. Ing.-Wes.* **1974**, *40*, 15−24.

Baehr, H. D.; Schomacker, H. Measurements of the specific isochoric heat capacity in the vicinity of the critical point of water. *Forsch. Ing.-Wes.* **1975**, *41*, 43−51.

Bright, F. V.; McNally, M. E. P., Eds. *Supercritical Fluid Technology*; ACS Symposium Series; American Chemical Society: Washington, DC, 1992.

Cooper, J. R. IAPWS Release on Skeleton Tables 1985 for the Thermodynamic Properties of Ordinary Water Substence. Physical chemistry of aqueous systems. Proceedings of the 12th International Conference on the Properties of Water and Steam; White, H., Sengers, J. V., Neumann, D. B., Bellows, J. C., Eds.; Begell House: New York, 1995; pp A13−83.

Franck, E. U. Physicochemical Properties of Supercritical Solvents. *Ber. Bunsen-Ges. Phys. Chem.* **1984**, *88*, 820−825.

Hanafusa, H.; Tsuchida, T.; Kawai, K.; Sato, H.; Uematsa, M.; Watanabe, K. Experimental Study of the PVT-Properties of Water in the Critical Region; Proceedings of the 10th International Conference on the Properties of Steam; Sychev, V. V., Aleksandrov, A. A., Eds.; MIR Publishers: Moscow 1986; Vol. 1, pp 180−191.

Hong, G. T.; Armellini, F. J.; Tester, J. W. Physical chemistry of aqueous systems. *Proceedings of the 12th International Conference on the Properties of Water and Steam.* White, H., Sengers, J. V., Neumann, D. B., Bellows, J. C., Eds.; Begell House: New York, 1995; pp 565.

Huang, S.; Daehling, K.; Carleson, T. E.; Abdel-Latif, M.; Taylor, P.; Wai, C. Propp, A. Supercritical Fluid Science and Technology. K. P. Johnson and J. M. L. Penninger, Eds. ACS, Washington, DC, **1989**. P.287.

Johnston, K. P., Penninger, J. M. L., Eds.; *Supercritical Fluid Science and Technology*; American Chemical Society Symposium Series 406; American Chemical Society: Washington, DC, 1989.

Kerimov, A. M. Ph.D. Thesis, Baku, Azerbajdjan, Azneftechim, 1964.

Kim, C.-H.; Vimalchand, P.; Donohue, M. D.; Sandler, S. I. Local compositions model for chainlike molecules: a new simplified version of the perturbed hard chain theory. *AIChE J.* **1986**, *32*, 1726−1734.

Kiran, E., Brennecke, J. F., Eds.; Supercritical Fluid Engineering Science. American Chemical Society Symposium Series 514; American Chemical Society: Washington, DC, 1993.

Kiran, E., Levelt Sengers, J. M. H., Eds.; S*upercritical Fluids Fundamentals for Application*; NATO ASI Series; Washington, DC, 1993; Vol. 273.

Kiselev, S. B.; Sengers, J. V. An improved parametric crossover model to the thermodynamic properties of fluids in the critical region. *Int. J. Thermophys.* **1993**, *14*, 1−31.

Kiselev, S. B.; Kostyukova, I. G.; Povodyrev, A. A. Universal crossover behaviour of fluids and fluid mixtures in the critical region. *Int. J. Thermophys.* **1991**, 12, 877−825.

Levelt Sengers, J. M. H. Supplementary Release on Saturation Properties of Ordinary Water Substance. Physical chemistry of aqueous systems. Proceedings of the 13th International Conference on the Properties of Water and Steam. White, H., Sengers, J. V., Neumann, D. B., Bellows, J. C., Eds.; Begell House: New York, 1995; pp A143−149.

Levelt Sengers, J. M. H.; Greer S. C. Thermodynamic Anomalies Near the Critical Point of Steam. *Int. J. Heat Mass Transfer* **1972**, *15*, 1865−1886.

Levelt Sengers, J. M. H.; Kamgar-Parsi, B.; Balfour, F. W.; Sengers, J. V. Thermodynamic properties of steam in the critical region. *J. Phys. Chem. Ref. Data.* **1983**, *12*, 1−28.

Luddecke, T. O.; Magee, J. W. Molar Heat Capacity at Constant Volume of R32 and R125 from the Triple-Point Temperature to 345 K at Pressure 35 MPa. *Int. J. Thermophys.* **1996**, *17*, 823−849.

Modell, M. Processing method for the oxidation of organics in supercritical water. U.S. Patent 4,543,190, 1985.

Osborne, N. S.; Stimson, H. F.; Fisck, E. F.; Ginnings, D. C. The Pressure of Saturated Water Vapor in the Range 100−374 °C. *J. Res. Natl. Bur. Stand. (U.S.)* **1933**, *10*, 155−188.

Preston-Thomas, H. The International Temperature Scale of 1990 (ITS-90). *Metrologia* **1990**, *27*, 3−10.

Sato, H.; Uematsu, M.; Watanabe, K. Propasal of the New Skeletori Tables for the Thermodynamic Properties of Water and Steam. Proceedings of the 10th International Conference on the Properties of Steam; Sychev, V. V., Aleksandrov, A. A., Eds.; MIR Publishers: Moscow, 1986; Vol. 1, pp 71−89.

Staszak, C. N.; Malinaaski, K. C.; Killilea, W. R. The pilot-scale demonstration of the MODAR oxidation process for the destruction of hazardous organic waste materials. *Envir. Prog.* **1987**, *6*, 39−43.

Tester, J. V.; Holgate, H. R.; Armellini, F. J.; Webley, P. A.; Killilea, W. R.; Hong, G. T.; Barner, H. E. Emerging technologies in hazardous waste management. Tedder, D. W., Pohland, F. G., Eds.; American Chemical Society: Washington, DC, 1991; p 35.

van Pelt A. Critical Phenomena in Binary Fluid Mixtures. Ph.D. Thesis, Netherland, 1992.

van Pelt, A.; Peters, C. J.; de Swaan J. A. Application of the simplified-perturbed-hard-chain Theory for pure components near the critical point. *Fluid Phase Equilib.* **1993**, *84*, 23−47.

Vargaftik, N. B. *Handbook of Physical Properties of Liquid and Gases*, 2nd ed.; Hemisphere: New York, 1983.

Voronel, A. V. Thermal measurements and critical phenomena in liquids. Phase Transitions and Critical Phenomena. Domb, C., Green, M. S., Eds.; Academic Press: London, 1974; Vol. 5, pp 343−394.

Wagner, W.; Saul, A. Correlation Equation for the Vapor Pressure and for the Orthobaric Densities of Water Substance. Proceedings of the 10th International Conference on the Properties of Steam; Sychev, V. V., Aleksandrov, A. A., Eds.; MIR Publishers: Moscow, 1986; Vol. 1, pp 199−209.

Weber, L. A. Measurements of the heat capacities $C_V$ of dense gaseous and liquid nitrogen and nitrogen trifluoride. *J. Chem. Thermodyn.* **1981**, *13*, 389−403.

Received for review February 11, 1998. Accepted June 8, 1998. The research was supported by the Russian Science Foundation under Grant Number 96-02-16005 and INTAS under Grant Number INTAS-96-1989.

JE980046W